IOSR Journal of Polymer and Textile Engineering (IOSR-JPTE)
e-ISSN: 2348-019X, p-ISSN: 2348-0181, Volume 13, Issue 2 (Mar. – Apr. 2026), PP 31-38
www.iosrjournals.org

Structural stability, Electronic and Optical Properties of Bulk MoS_2 Transition Metal Dichalcogenides: A DFT Approach

Shehu Aminu Yamusa[1,*], Amiruddin Shaari[2], Ibrahim Isah[3]
[1]*Department of Physics, Faculty of Science, Universiti Teknologi Malaysia*
[2]*Department of Physics, Faculty of Science, Federal College of Education, Zaria*
[3]*Department of Science and Laboratory Technology, Jigawa State Polytechnic, Dutse*
Correspondence Author: aminuyamusa56@gmail.com*

Abstract: *This paper investigates the structural stability, electronic, and optical properties of MoS_2 in hexagonal and trigonal phases using the first-principles method, the results show that the two-phase bulk $MoS_2$is stable. The material has a bandgap of 1.37eV and 1.52eV in hexagonal and trigonal phases which are in agreement with the available literature and also indicated that both phases of the materials are semiconductors. The work shows the materials have a potential for use in optoelectronic applications due to their significant response to incident radiation*

Keywords: *DFT, Transition metal dichalcogenides, external field, chalcogen, optical properties*

I. Introduction

Graphene is a hexagonal carbon sheet with a two-dimensional structure [8]. But its lack of an electronic bandgap limits its application areas and sparked a hunt for 2D materials with semiconducting capabilities [9, 10]. Transition metal dichalcogenides (TMDCs) are semiconductors of the form MX_2,with M a transition-metal atom (Mo, W, etc.) and X a chalcogen atom (S, Se, or Te)[11]. One layer of M atoms between two layers of X atoms.Two-dimensional dichalcogenides have a new window due to the new advantage in nanoscale materials. MX2 (MoS_2, $MoSe_2$) is a type of MX_2.[12] WS_2 and WSe_2[13].MoS_2 is a semiconductor with a direct band gap at the monolayer level and an indirect band gap at the bulk level. The band gaps of these materials fall between 400 and 700 nanometers in the visible section of the electromagnetic spectrum. MoS_2 is a common transition metal disulfide (TMD) frequently employed in many energy applications. Chen et al. [14] study the structure, electronic and optical properties of WS2 disulfide using DFT. They considered hexagonal (P63/*mmc*) and rhombohedral (R3m) structures, where they reported WS2 to be thermodynamically and dynamically stable. In a recent study by Nguyen et al.[15] where they examined the electrical and optical properties of the hexagonal structure of the Bulk and monolayer MoS2 crystals, utilizing APW +Lo method; they reported energy bandgaps of 1.23 eV and 1.70 eV, respectively. Ahmad et al. [15] used a self-consistent plane-wave pseudopotential total energy method based on the DFT technique implemented in Quantum Espresso code to study bulk and monolayered MoS_2 Their result shows that the calculated lattice parameters overestimate the experimental values, which is an inherent feature of standard GGA functional; the finding also shows that the bulk and monolayer bandgaps are 0.89 and 1.57 eV, respectively, which differ from experimental values of 1.29 and 1.80 respectively[16, 17].

In recent years, numerous studies have been conducted on the optical properties of TMDCs. include spectrum reflectance, differential reflectance, transmittance, spectral absorption, and absorbance among others. Lahourpour et al. [41] similarly observed a high anisotropic response in the infrared up to the beginning of the ultraviolet region. At the same time, Hieu et al. saw an isotropic response at higher energies.

However, recent research on MoS_2 has focused mostly on the monolayer structure, even though the bulk material has yet to be understood fully, this includes less work on electrical and optical properties of the bulk system among others. In addition, previous research revealed this material to have two polymorphs (phases), the hexagonal phase (P63/mmc (194)) and trigonal phase (P3m1 (164)) with the hexagonal phase extensively studied and little work forthe trigonal phase. The present work aims to determine the structural stability, and electronic and optical properties of the two polymorphs of MoS_2, these include among others the equilibrium lattice parameters, Born stability criteria, phonon dispersion curve, band gap, and density of the state.

II. Methodology

To investigate the structural stability and optical properties of hexagonal $P6_3/mmc$[194] and trigonal $P\bar{3}m1$[164]. We used the first-principle plane wave method based on density functional theory (DFT) implemented by the Quantum Espresso package[20]. employing ultra-soft pseudopotential and the Perdew-Burke –Ernzerhof (PBE) exchange-correlation energy function with the generalized gradient approximation (GGA)[1]To sample the first Brillion zone (BZ), a (8 x 8 x 2) k-mesh monkhorst-pack grid is used. We employed a 8 x 8 x 2 k-mesh monkhorst-pack grid for the density of state and a 12 x 12 x 3 grid for the optical plane-wave basis properties and using 400 eV as the kinetic energy cutoff.Thermo_pw package, a Q.E. plugin[1], was used for phonon dispersion and optical properties calculations. Finally, for the phonon dispersion,we employed a 12 x 12 x 12 K-mesh monkhorst-pack grid with norm-conserving pseudopotentials.

III. Results and discussion

3.1. Structural parameters

The total energy versus volume of the materials in their non-magnetic phases is determined to analyze the structural characteristics of the MoS2 material. Our findings demonstrate the stability of these materials in the non-magnetic phase.[23] Molybdenum disulfide has a hexagonal $P6_3/mmc$[194] and trigonal $P\bar{3}m1$[164] the structure consists of Mo and S layers, as shown in Fig.(1.1a) and Fig.(1.1b), respectively. The Bulk MoS_2 has two such layers, and Mo atoms of one layer are directly above the Sulphur atoms of the other layer and vice-versa. After relaxation, we obtained the calculated structural parameters of hexagonal and trigonal Bulk MoS_2 using GGA, as shown in Table (1.1). With recently calculated values using projected augmented plane wave (PAW). We find excellent agreements with PAW-based calculations. The calculated lattice parameters for both hexagonal and trigonal Bulk MoS_2 were in good agreement with other available literature, though, the functional applied (GGA) generally overestimates the experimental values, which is an inherent feature of the functionals.Structural parameters of Bulk MoS_2 with GGA are in excellent agreement with experimentally measured values, although there is a slight underestimation. our result shows that the equilibrium volume of trigonal is larger than the hexagonal

3.2 Structural Properties

(a) (b)

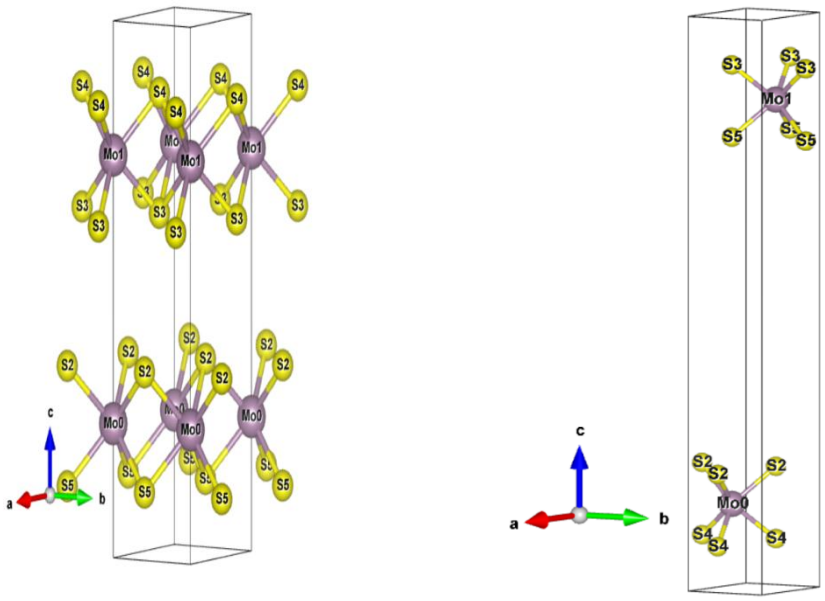

Figure 1.1 MoS_2 Structure in (a) Hexagonal $P6_3/mmc$ [194] phase and (b) Trigonal $P\bar{3}m1$[164]phase MoS_2

Table 1.1 Calculated equilibrium Lattice parameters, volume, Bulk Modulus, and pressure derivatives of hexagonal and trigonal Bulk MoS_2

Bulk MoS2	XC	a (Å)	c (Å)	V (Å^3)	B0 (Gpa)	$B_0^{'}$	Ref.
hexagonal $P6_3/mmc[194]$	GGA	3.08	13.09	119.41	128.8	4.47	This work
	GGA	3.19	12.31				[15]
	Exp	3.16	12.29				[24]
trigonal $P\bar{3}m1[164]$	GGA	3.08	21.47	194.51	76.6	4.56	This work

Table 1.2 Calculated bandgap of hexagonal and trigonal Bulk of MoS2

Bulk MoS_2	XC	Bandgap (eV)	Ref.
hexagonal $P6_3/mmc[194]$	GGA	$1.37[K-\Gamma]$	This work
		1.23	[25]
		1.29	[26]
		0.89	[15]
trigonal $P\bar{3}m1[164]$	GGA	$1.56[K-\Gamma]$	This work

The energy versus volume plot for the two phases was produced by fitting energy against volume in the Murgahans equation of the state. fig.1.2. The structural constants, besides other theoretical reports, are illustrated in table 1.1. The calculated Bulk modulus o , volume V and pressure derivative $B_0^{'}$Represented in table1.1. Both phases have almost the same ground state energy with equilibrium volumes of 119.41and 194.51 Å^{3,} for hexagonal and trigonal phases respectively

3.3StructuralStability

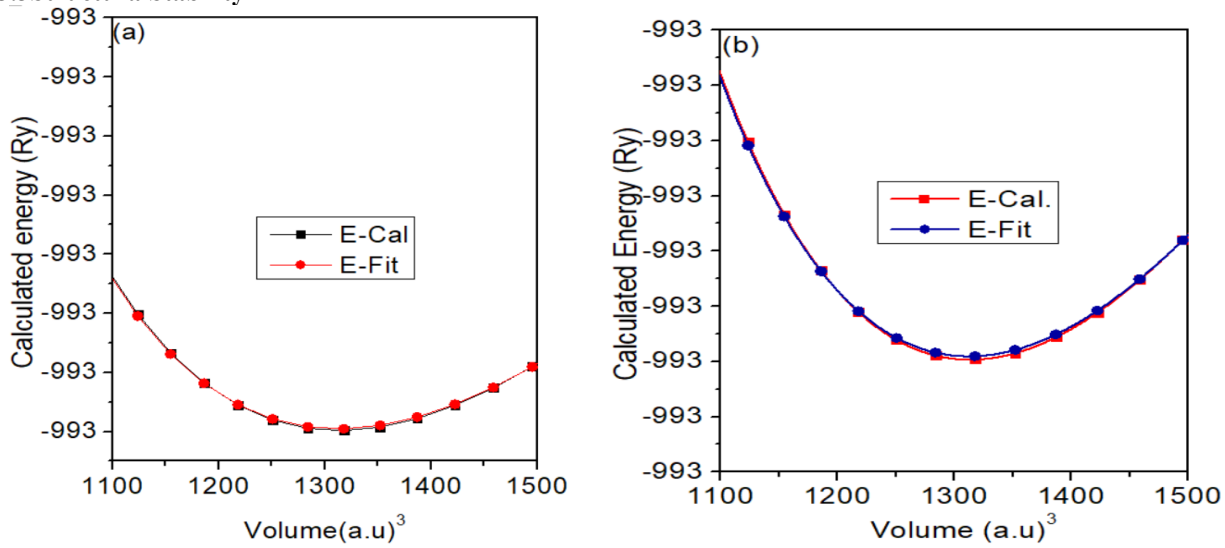

Figure 1.2 Energy volume curves (a) hexagonal $P6_3/mmc$ *(194)* (b) Trigonal Bulk MoS_2 $P\bar{3}m1[164]$

The mechanical stability of hexagonal and trigonal structures was checked using the Born stability criteria.

$$C_{11} > 0, C_{33} > 0, C_{44} > 0, \quad (1.1)$$
$$(C_{11} - C_{12}) > 0, \quad (1.2)$$
$$(C_{11} + C_{12}) > C_{33} - 2C_{13}^2 > 0, \quad (1.3)$$

Both systems are mechanically stable. However, the study of the dynamical stability of these compounds using the phonon dispersion curve confirmed no imaginary frequency in both systems, as shown in figure 1.3 below; therefore, the two systems are mechanically and dynamically stable.

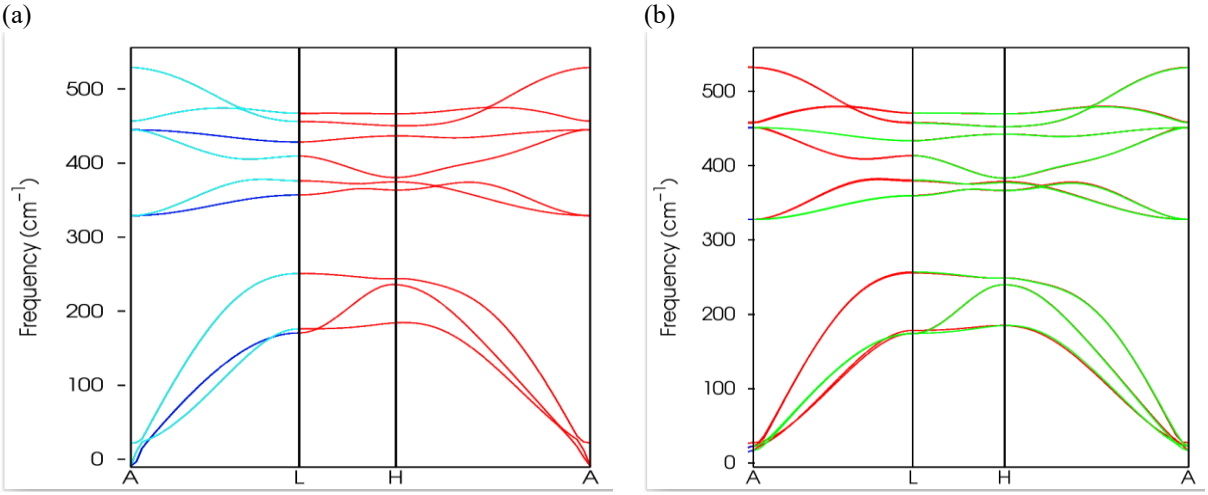

Figure:1.3 Phonon Dispersion curves (a) Hexagonal MoS_2 and (b) Trigonal MoS_2

3.4Electronic Band structure and density of states

The electronic band structure and corresponding density of states diagram for *the hexagonal* and trigonal bulk MoS_2 are shown in Fig.1.3(a) and Fig.1.3(b), respectively, The density of states for both hexagonal and trigonal Bulk moS2 are in four groups of occupied and unoccupied states, separated by gaps. In the first group, bands in the electronic band structure and density of states around -7.59 to -1.00 eV are mainly due to the 3p orbital and 4d orbital of S and Mo atoms. The second group above Fermi energy ranges from -1.00 to 0.77 eV, with 3p orbital of S and 4d orbital of Mo mainly contributing. In the third group above the Fermi energy, the energy range is between 0.56 to 4.75 eV; the main contribution is due to 4d orbitals of Mo and 3p of S mainly contributing and showing strong hybridization. Lastly above 5.22 eV contributes to the lowest conduction bands, mainly 5s and 3s of Mo and S orbitals.

The bands around the bandgap are relatively flat, as expected from the 'd' character of the electron states at these energies. In both phases of MoS_2, the valence band maximum is at*Γ*the conduction band minimum is between K and *Γ*revealing an indirect band semiconductor, as seen in Fig.1.4 and Fig.1.5

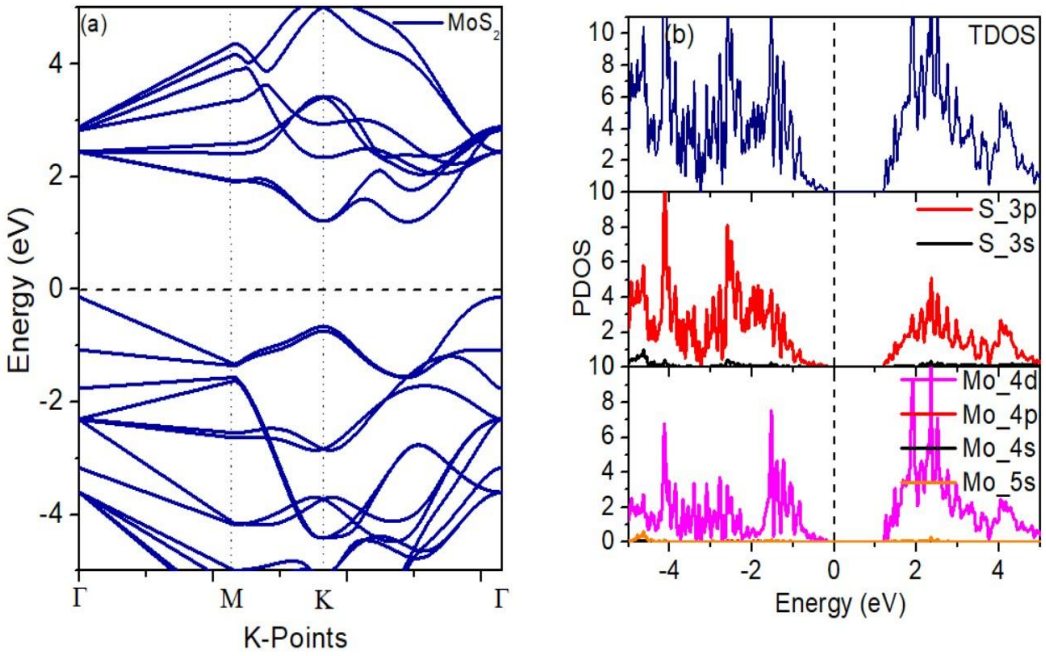

Figure 1.4 the calculated electronic band and density of states of MoS_2 using GGA (a) the electronic bandgap of hexagonal MoS_2. (b) the density of state of hexagonal MoS2of state of hexagonal MoS2

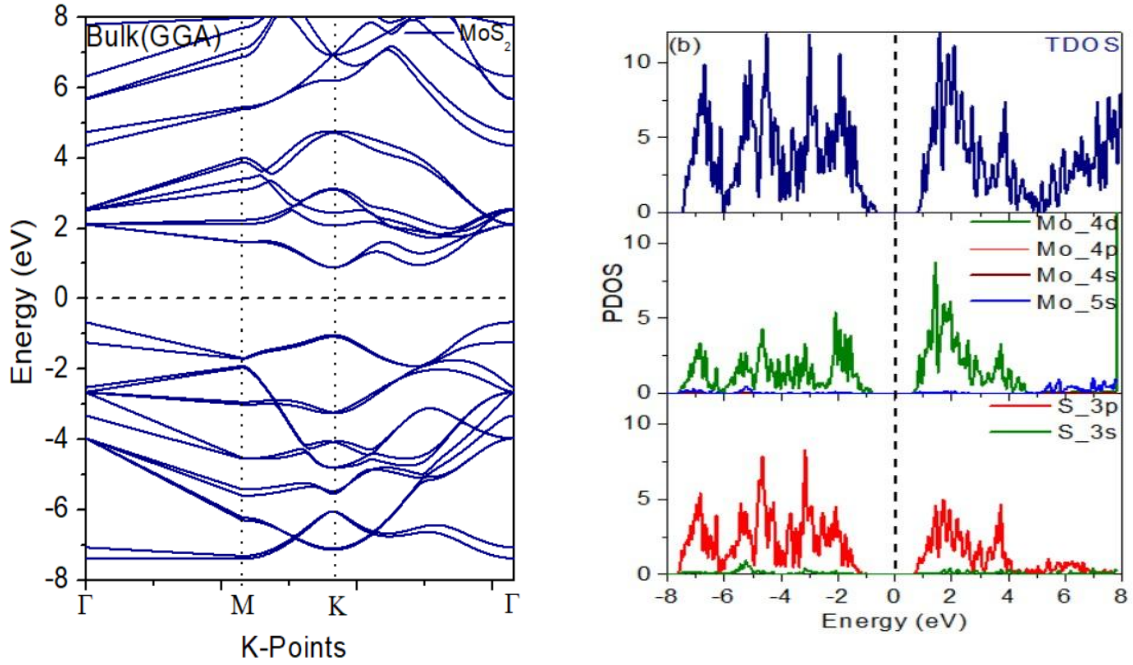

Figure 1.5 the calculated electronic band and density of states of MoS_2 using GGA (a) the electronic bandgap of trigonal MoS_2. (b) the density of state of trigonal MoS_2

The calculated electronic bandgap for both *hexagonal* and trigonal phases of bulk $MoS_2$is presented above in Table 1.2. Although our calculated band gaps for bulk MoS_2 are in good agreement with other theoretical values [25, 26], but underestimate the experimental band gap due to the inherent drawback of standard LDA/GGA functionals. Our calculated value of electronic band gap for *hexagonal* $P6_3$/mmc bulk MoS_2 using GGA is 1.37 eV and trigonal bulk MoS_2 using GGA 1.52 eV, respectively, which is in excellent agreement with [25-28].

3.5. Optical properties

Understanding Light interactions with materials are significant for optoelectronic device applications. Materials that have significant responses to incident radiation are good candidates, dielectric constant described these characteristics. It is possible to calculate the dielectric properties of a compound with hexagonal or trigonal symmetry when the electric vector E is perpendicular to or parallel to the c axis. [29]. This research focuses ontime-dependent density-functional theory (TDDFPT) and linear response technique, using the Sternheimer approach by the Thermo_ pw code, a proprietary branch of the QUANTUM ESPRESSO project[30]. The calculated real and imaginary parts of the frequency-dependent macroscopic dielectric functionwithin the energy range 0 to 21 eV are plotted in Figures 3.0 and 3.1, respectively. Direct electronic transitions between occupied and unoccupied electronic states were used to derive the imaginary portion of the dielectric function, which was then calculated using equation eq.1[2], the real part of a macroscopic dielectric function describes how much material has been polarised due to induced electric dipole creation by an external field, and the real dielectric function can be derived from the Kramers-Kroning relationship[3]

$$\varepsilon_2(\omega) = \frac{2\pi e^2}{\Omega\varepsilon_0}\sum_{k,v.c}\left|\vec{\lambda}.\langle\psi_k^c|u.r|\psi_k^v\rangle\right|^2\delta(E_k^c - E_k^v - E) \quad (1)$$

Here, the integral is over the Brillouin zone, u,ωe,ψ_k^c,ψ_k^v are the polarization vector of the incident electric field, frequency of light, the electronic charge, and conduction and valance band wave function at k respectively.

$$\varepsilon_1(\omega) = 1 + \frac{2}{\pi}P\int_0^\infty \frac{\omega'\varepsilon_2(\omega')}{\omega' - \omega^2}d\omega' \quad (2)$$

Where P stands for the principle value of the itegralAs we can see in fig.1.7a and fig.1.7b, the hexagonal structure is sharper and more vivid than the trigonal form. The maximum real and imaginary peaks for Hexagonal and trigonal are presented in table 1.3 MoS2. From hexagonal to trigonal, the value of the real part at

zero increases, and the real part of the dielectric function shows instability in the optical response at the range of The earlier theoretical and experimental findings are consistent with the current work[4-7].

Table 1.2 Calculated real and imaginary dielectric function of hexagonal and trigonal Bulk of MoS2		
System	Real part	Imaginary part
Hexagonal $P6_3/mmc$[194]	$\varepsilon_{xx}(0)$=14.93 $\varepsilon_{zz}(0)$=8.19 $\varepsilon_{xx}^{max}(\omega)$=24.38(1.87eV) $\varepsilon_{zz}^{max}(\omega)$=16.25(4.53eV)	$\varepsilon_{xx}^{max}(\omega)$=25.33 (2.55 eV) $\varepsilon_{zz}^{max}(\omega)$=17.79 (5.46 eV)
Trigonal $P\bar{3}m1$[164]	$\varepsilon_{xx}(0)$=5.54 $\varepsilon_{zz}(0)$=3.26 $\varepsilon_{xx}^{max}(\omega)$=9.11 (2.03 eV) $\varepsilon_{zz}^{max}(\omega)$=6.39 (4.78 eV)	$\varepsilon_{xx}^{max}(\omega)$=9.09 (2.55 eV) $\varepsilon_{zz}^{max}(\omega)$=7.24 (5.55 eV)

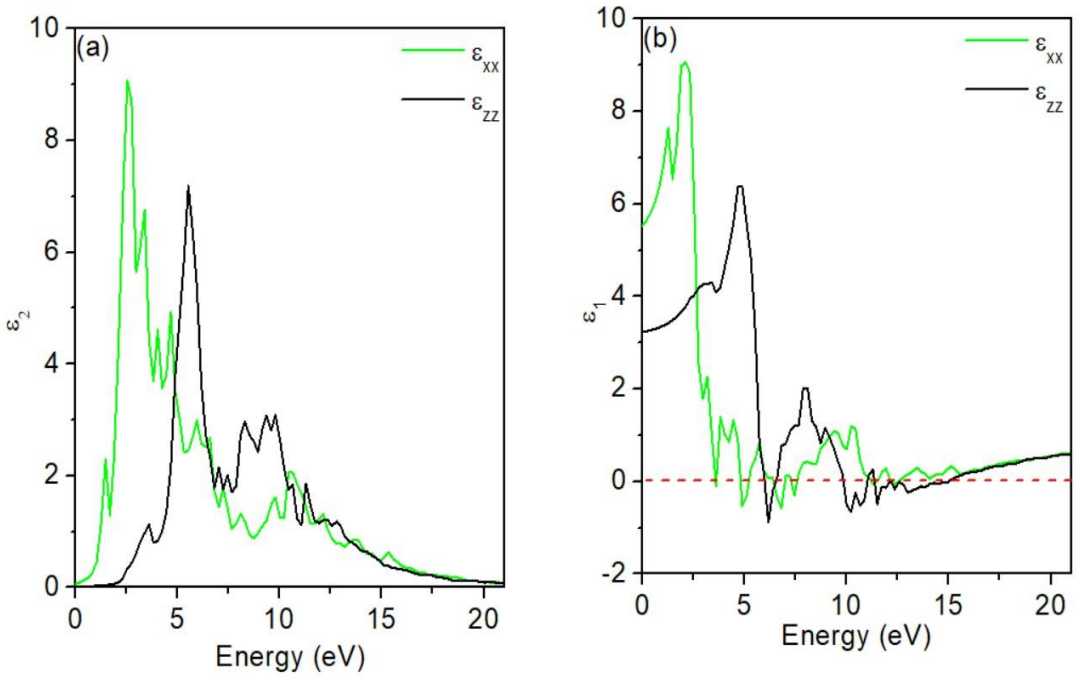

Figure 1.7 the calculated dielectric constant of MoS_2 using GGA (a) the imaginary part of trigonal MoS_2. (b) the real of trigonal MoS_2

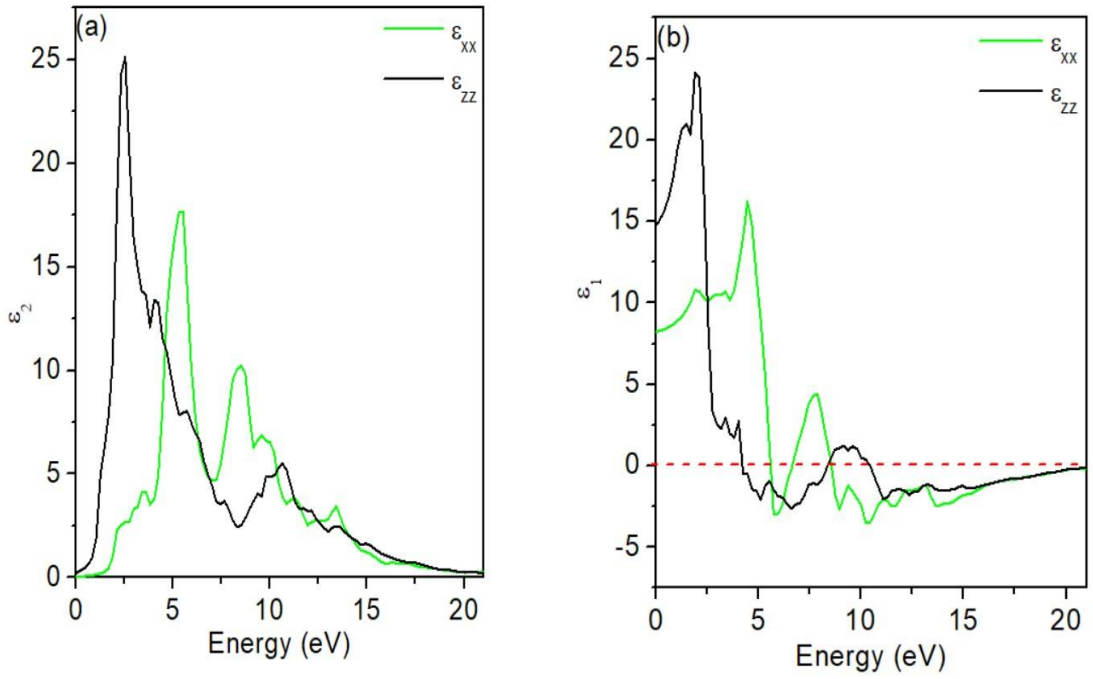

Figure 1.8 the calculated dielectric constant of MoS_2 using GGA (a) the imaginary part of hexagonal MoS_2. (b) the realof hexagonal MoS_2

IV. Conclusion

In conclusion, the structural, electrical, and optical characteristics of MoS_2 were investigated using the first principles method. In this regard, it has been found that the stability level increases from hexagonal which shows that boh Polymorphs of the crystal MoS_2 are stable, they are both semiconductors with an indirect band gap between 1-1.5eV, which agrees well with previous theoretical and experimental findings. The results show that the bandgap of the trigonal is larger than hexagonal. Lastly, our findings in the optical properties the real and the imaginary part of hexagonal is larger than the real and the imaginary part of the dielectric function of trigonal.

References

[1]. Du, J., et al., *Strain engineering in 2D material-based flexible optoelectronics.* Small Methods, 2021. **5**(1): p. 2000919.
[2]. Yang, S.-H., et al., *Chiral spintronics.* Nature Reviews Physics, 2021. **3**(5): p. 328-343.
[3]. *<Quasiparticle Band Structures of Bulk and Few-layer PdSe2 from First-principles GW Calculations.pdf>.*
[4]. Guan, Z., et al., *Recent Progress in Two-Dimensional Ferroelectric Materials.* Advanced Electronic Materials, 2019. **6**(1).
[5]. Kumar, A. and P.K. Ahluwalia, *A first principle Comparative study of electronic and optical properties of 1H – MoS2 and 2H – MoS2.* Materials Chemistry and Physics, 2012. **135**(2-3): p. 755-761.
[6]. Chen, X., et al., *Recent advances in fluorinated graphene from synthesis to applications: Critical review on functional chemistry and structural engineering.* Advanced Materials, 2022. **34**(1): p. 2101665.
[7]. Sun, L., et al., *Hetero-site nucleation for growing twisted bilayer graphene with a wide range of twist angles.* Nature communications, 2021. **12**(1): p. 1-8.
[8]. Neto, A.C., et al., *The electronic properties of graphene.* Reviews of modern physics, 2009. **81**(1): p. 109.
[9]. Panigrahi, P., et al., *Elemental Substitution of Two-Dimensional Transition Metal Dichalcogenides (MoSe2 and MoTe2): Implications for Enhanced Gas Sensing.* ACS Sensors, 2019. **4**(10): p. 2646-2653.
[10]. Choi, W., et al., *Synthesis of Graphene and Its Applications: A Review.* Critical Reviews in Solid State and Materials Sciences, 2010. **35**(1): p. 52-71.
[11]. Ugeda, M.M., et al., *Giant bandgap renormalization and excitonic effects in a monolayer transition metal dichalcogenide semiconductor.* Nature materials, 2014. **13**(12): p. 1091-1095.
[12]. Ahmad, I., et al., *Influence of strain on specific features of MoX2 (X= S, Se, Te) monolayers.* Physica B: Condensed Matter, 2018. **545**: p. 113-118.
[13]. Muoi, D., et al., *Electronic properties of WS2 and WSe2 monolayers with biaxial strain: a first-principles study.* Chemical Physics, 2019. **519**: p. 69-73.
[14]. Chen, S., et al., *Structural Stability and Electronic and Optical Properties of Bulk WS2 from First-Principles Investigations.* Journal of Electronic Materials, 2020. **49**(12): p. 7363-7369.
[15]. Ahmad, S. and S. Mukherjee, *A Comparative Study of Electronic Properties of Bulk MoS2 and Its Monolayer Using DFT Technique: Application of Mechanical Strain on MoS2 Monolayer.* Graphene, 2014. **03**: p. 52-59.
[16]. Böker, T., et al., *Band structure of ${\mathrm{MoS}}_{2},$ ${\mathrm{MoSe}}_{2},$ and $\ensuremath{\alpha}\ensuremath{-}{\mathrm{MoTe}}_{2}:$ Angle-resolved photoelectron spectroscopy and ab initio calculations.* Physical Review B, 2001. **64**(23): p. 235305.

[17]. Mak, K.F., et al., *Atomically Thin ${\mathrm{MoS}}_{2}$: A New Direct-Gap Semiconductor.* Physical Review Letters, 2010. **105**(13): p. 136805.
[18]. Bagayoko, D., *Understanding density functional theory (DFT) and completing it in practice.* AIP Advances, 2014. **4**(12): p. 127104.
[19]. Giannozzi, P., et al., *Advanced capabilities for materials modelling with Quantum ESPRESSO.* Journal of Physics: Condensed matter, 2017. **29**(46): p. 465901.
[20]. Giannozzi, P., et al., *Quantum ESPRESSO toward the exascale.* The Journal of Chemical Physics, 2020. **152**(15): p. 154105.
[21]. Dufek, P., P. Blaha, and K. Schwarz, *Applications of Engel and Vosko's generalized gradient approximation in solids.* Physical Review B, 1994. **50**(11): p. 7279.
[22]. Monkhorst, H.J. and J.D. Pack, *Special points for Brillouin-zone integrations.* Physical Review B, 1976. **13**(12): p. 5188.
[23]. Zhang, H., et al., *Engineering magnetic properties of Ni nanoparticles by non-magnetic cores.* Chemistry of materials, 2009. **21**(21): p. 5222-5228.
[24]. Wilson, J.A. and A.D. Yoffe, *The transition metal dichalcogenides discussion and interpretation of the observed optical, electrical and structural properties.* Advances in Physics, 1969. **18**(73): p. 193-335.
[25]. Hieu, N.N., et al., *First-principles study of optical properties of molybdenum disulfide: From Bulk to monolayer.* Superlattices and Microstructures, 2018. **115**: p. 10-18.
[26]. Böker, T., et al., the *Band structure of MoS 2, MoSe 2, and α− MoTe 2: Angle-resolved photoelectron spectroscopy and ab initio calculations.* Physical Review B, 2001. **64**(23): p. 235305.
[27]. Ataca, C., et al., *Mechanical and electronic properties of MoS2 nanoribbons and their defects.* The Journal of Physical Chemistry C, 2011. **115**(10): p. 3934-3941.
[28]. Ahmad, S. and S. Mukherjee, *A comparative study of electronic properties of Bulk MoS2 and its monolayer using DFT technique: application of mechanical strain on MoS2 monolayer.* 2014.
[29]. Perdew, J.P., K. Burke, and M. Ernzerhof, *Generalized gradient approximation made simple.* Physical review letters, 1996. **77**(18): p. 3865.
[30]. Lawal, A., et al., *Sb2Te3/graphene heterostructure for broadband photodetector: A first-principles calculation at the level of Cooper's exchange functionals.* Optik, 2019. **177**: p. 83-92.
[31]. Onida, G., L. Reining, and A. Rubio, *Electronic excitations: Density-functional versus many-body Green's-function approaches.* Reviews of Modern Physics, 2002. **74**(2): p. 601-659.
[32]. Beal, A. and H. Hughes, *Kramers-Kronig analysis of the reflectivity spectra of 2H-MoS2, 2H-MoSe2 and 2H-MoTe2.* Journal of Physics C: Solid State Physics, 1979. **12**(5): p. 881.
[33]. Beal, A., H. Hughes, and W. Liang, *The reflectivity spectra of some group VA transition metal dichalcogenides.* Journal of physics C: solid state physics, 1975. **8**(24): p. 4236.
[34]. Lahourpour, F., et al., *Structural, electronic and optical properties of graphene-like nano-layers MoX2(X:S,Se,Te): DFT study.* Journal of Theoretical and Applied Physics, 2019. **13**(3): p. 191-201.
[35]. Hieu, N.N., et al., *First principles study of optical properties of molybdenum disulfide: From bulk to monolayer.* Superlattices and Microstructures, 2018. **115**: p. 10-18.